Tailored phase conversion under conjugated polymer enables thermally stable perovskite solar cells with efficiency exceeding 21%

Lei Meng[†,‡], Chenkai Sun[‡], Rui Wang[†], Wenchao Huang[†,§], Zipeng Zhao[†], Pengyu Sun[†], Tianyi Huang[†], Jingjing Xue[†], Jin-Wook Lee[†], Chenhui Zhu[‖], Yu Huang[†], Yongfang Li[‡,*], and Yang Yang[†,*]

[†]Department of Materials Science and Engineering, University of California, Los Angeles, California 90095, United States.

[‡]Beijing National Laboratory for Molecular Sciences, CAS Key Laboratory of Organic Solids, Institute of Chemistry, Chinese Academy of Sciences, Beijing 100190, China.

[§]Department of Materials Science and Engineering, Monash University, Wellington Road, Clayton, VIC 3800, Australia.

[‖]Advanced Light Source, Lawrence Berkeley National Laboratory, Berkeley, California 94720, United States.

Experimental details

Materials. The SnO_2 colloid dispersion (tin (IV) oxide) was purchased from Alfa Aesar. PbI_2, PTAA, chloroform (anhydrous), toluene (anhydrous), N,N-dimethylformamide (DMF), and dimethyl sulfoxide (DMSO) were purchased from Sigma-Aldrich. Formamidinium iodide (FAI), methylammonium bromide (MABr), and methylammonium chloride (MACl) were purchased from Dyesol. 4-Isopropyl-4'-methyldiphenyliodonium Tetrakis(pentafluorophenyl)borate (TPFB) was obtained from TCI America.

Device fabrication. Indium doped tin oxide (ITO) glass was cleaned with sequential sonication in detergent, deionized (DI) water, acetone and 2-propanol for 15 min, respectively. The cleaned substrates were treated with UV-ozone for 20 min before use. The SnO_2 colloid dispersion was

diluted with DI water as ratio of 1:6 and the dispersion was filtered by 0.2 μm syringe filter. To form a compact SnO_2 layer, the solution was spin-coated on the cleaned ITO substrate at 3000 rpm for 30 s and the film was annealed at 150 °C for 30 min. The substrates were cooled down in air before use. For the fabrication of bare perovskite, 1.5 M of PbI_2 in (DMF:DMSO = 93:7 in volume ratio) was spin coated onto SnO_2 at 1500 rpm for 30 s and annealed at 75°C for 2 min. The organic halide solution of FAI:MABr:MACl was prerpared in 1 mL 2-propanol with ratio of 70 mg : 7 mg : 8 mg and then spin-coated onto the PbI_2 after cooling down. The thermal annealing was conducted in air at 150 °C for 10 min. For polymer-treated perovskite, 10 mg/mL of PTQ10 dissolved in chloroform was spin-coated on the PbI_2/FAI adduct film at 2500 rpm right before thermal annealing of perovskite. PTAA and dopant TPFB was dissolved in toluene with the concentration of 30 mg/mL and the solution was spin-coated at 2000 rpm for 30 s. 100 nm-thick silver was thermally evaporated at 0.5 Å/s as electrode.

Materials characterization. UV-vis absorption spectra were recorded by U-4100 spectrophotometer (Hitachi) equipped with integrating sphere. The perovskite layer was coated on ITO substrate for the measurements. A field-emission scanning electron microscope (FEI Nova 230 NanoSEM) was used to acquire surface and cross-sectional SEM images. The instrument used an electron beam accelerated at 500 V to 30 kV, enabling operation at a variety of currents. GIWAXS experiment were conducted at the beamline 7.3.3 of the Advanced Light Source at Lawrence Berkeley National Laboratory. All the samples were irradiated by 10 KeV X-ray at a fixed angle of 0.3°. 2D scattering signals were probed by using a Dectris Pilatus 1M detector. The results were analyzed by an altered version of the NIKA 2D based in IgorPro. Steady-state photoluminescence (PL) was measured using a Horiba Jobinyvon system with excitation at 600 nm. In the TRPL measurement, the samples were excited by a pulsed laser (PDL 800-B system with an external trigger), with a wavelength and frequency of 632 nm and 1 MHz, respectively. The photoluminescence photons were counted by a Picoharp 300 after being pre-amplified by a pre-amplifier module (PAM102, PicoQuant). XPS measurements were carried out on an XPS

AXIS Ultra DLD (Kratos Analytical). An Al Kα (1,486.6 eV) X-ray was used as the excitation source. UPS measurements were carried out to determine the work function and the position of valence band maximum of materials. A He discharge lamp, emitting ultraviolet energy at 21.2 eV, was used for excitation. All UPS measurements were performed using standard procedures with a −7 V bias applied between the samples and detectors. Clean gold is used as a reference. High angle annular dark field scanning transmission electron microscopy (HAADF STEM) images, EDS maps and line scan profiles were taken on a JEOL 2800 TEM/STEM operated at 200 kV. The device glass/ITO/SnO_2/perovskite/HTL/Ag was used for the TEM sample. The focused ion beam technique was used for cross-TEM sample preparation.

Device characterization. Current density-voltage (J-V) curves of the devices were measured using Keithley 2401 source meter under simulated one sun illumination (AM 1.5G, 100 $mWcm^{-2}$). The one sun illumination was generated from Oriel Sol3A with class AAA solar simulator (Newport), in which light intensity was calibrated by Si photodiode equipped with KG-2 filter. Typically, the devices were measured in reverse scan (1.2 V ⟶ 0 V, step 0.02 V) and forward scan (0 V ⟶ 1.2 V, step 0.02 V). All the devices were measured without pre-conditioning such as light-soaking and applied bias voltage. Steady-state power conversion efficiency was calculated by measuring stabilized photocurrent density under constant bias voltage. The external quantum efficiency (EQE) was measured using specially designed system (Enli tech) under AC mode (frequency=133 Hz) without bias light. For transient photovoltage (TPV) and current (TPC) measurements, a white light bias was generated from an array of diodes (Molex 180081-4320) to simulate 0.5 sun bias light working condition. A pulsed red dye laser (Rhodamine 6G, 590nm) pumped by a nitrogen laser (LSI VSL-337ND-S) was used as the perturbation source, with a pulse width of 4 ns and a repetition frequency of 10 Hz. The intensity of the perturbation laser pulse was controlled to maintain the amplitude of transient VOC below 5 mV so that the perturbation assumption of excitation light holds. The voltages under open circuit and currents under short circuit conditions were measured over a 1 MΩ and a 50 Ω resistor, and were recorded on a digital

oscilloscope (Tektronix DPO 4104B).

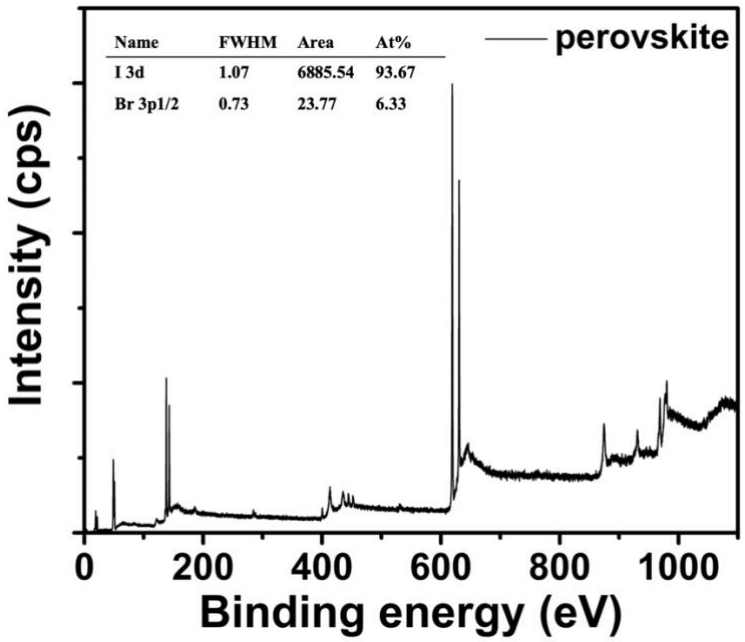

Figure S1. X-ray photoelectron spectroscopy (XPS) analysis to determine the stoichiometric ratio of I and Br in the final perovskite film.

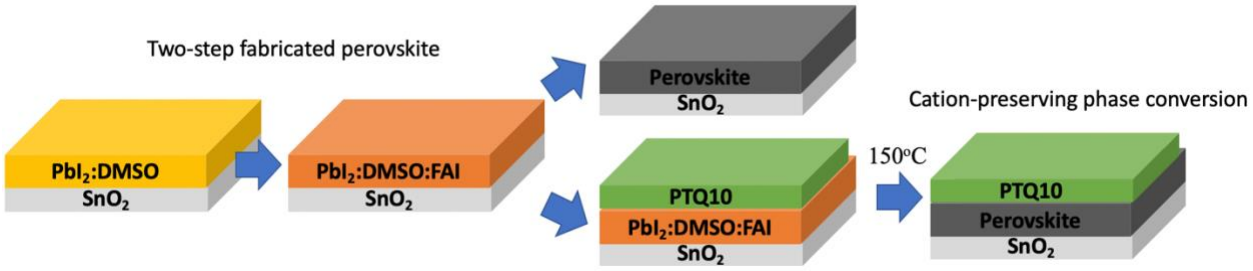

Figure S2. Schematic demonstration of the regular two-step method and cation-preserving phase conversion process of $FAPbI_3$ film fabrication.

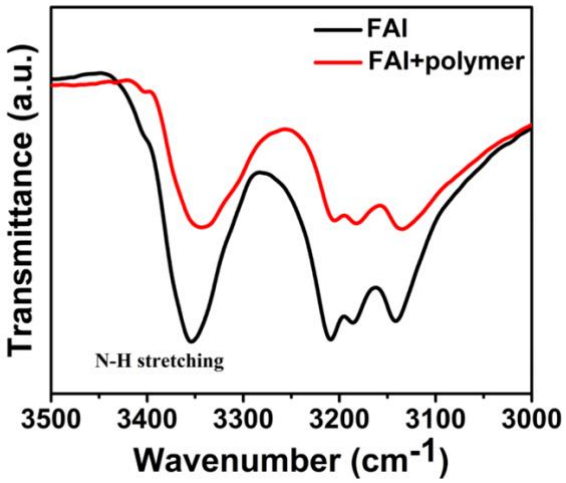

Figure S3. Fourier transform infrared spectra for the fingerprint region of N-H stretching in the case of pure FAI and FAI incorporating polymer. The peak N-H stretching red-shifted by around 9 cm^{-1} after incorporating PTQ10 compared with the bare FAI.

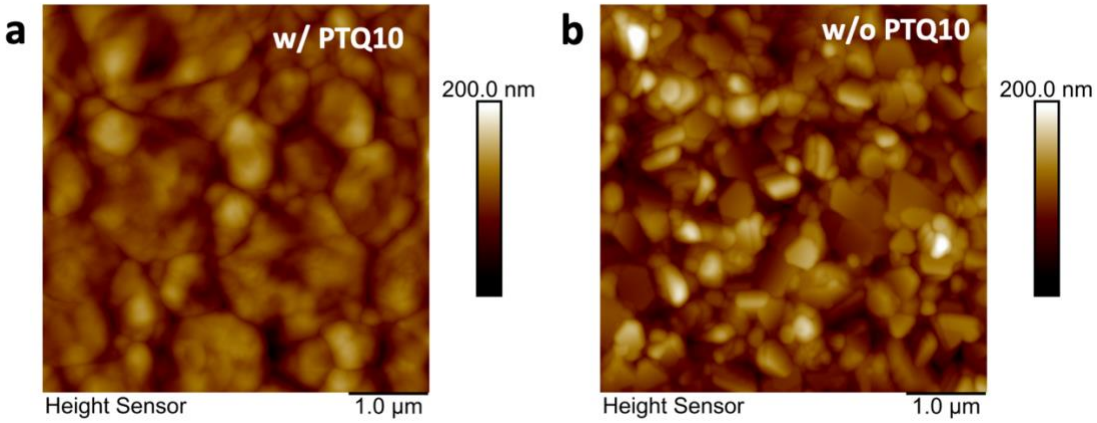

Figure S4. Atomic force microscopy (AFM) images for (a) perovskite film treated with PTQ10 and (b) control film.

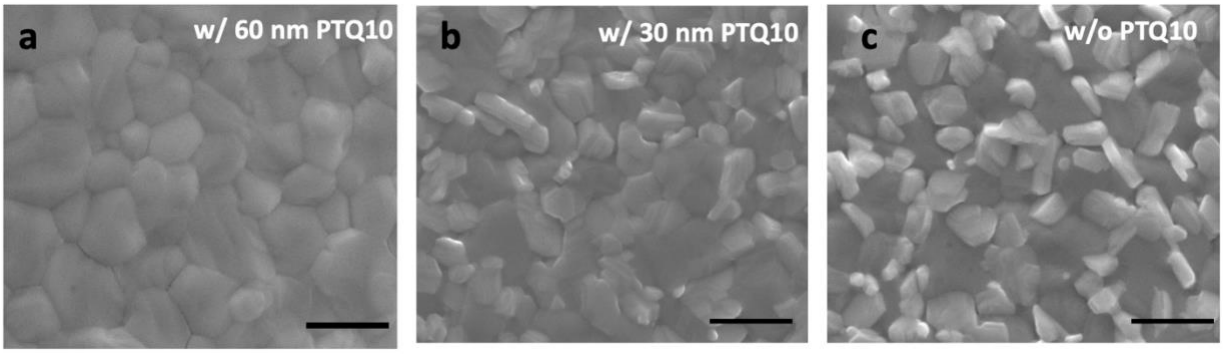

Figure S5. The SEM images of perovskite films treated with (a) PTQ10 with thickness of 60 nm and (b) PTQ10 with thickness of 30 nm. The scale bar in the figures represents length of 1 μm. For the perovskite films treated with PTQ10, the polymer was completely washed away by soaked into chloroform before the SEM analysis. (c) Traditional perovskite film fabricated through two-step method.

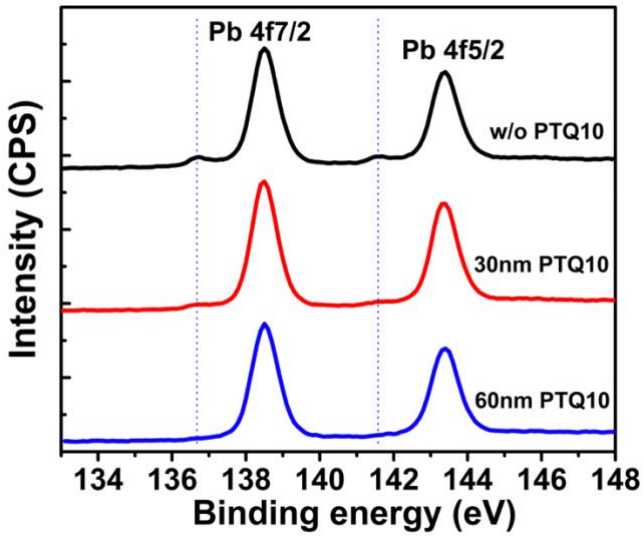

Figure S6. X-ray photoelectron spectroscopy (XPS) characterization of 4f7/2 and 4f5/2 spectra of Pb element on the surface of perovskite films with treatment of different PTQ10 thickness (30nm and 60 nm).

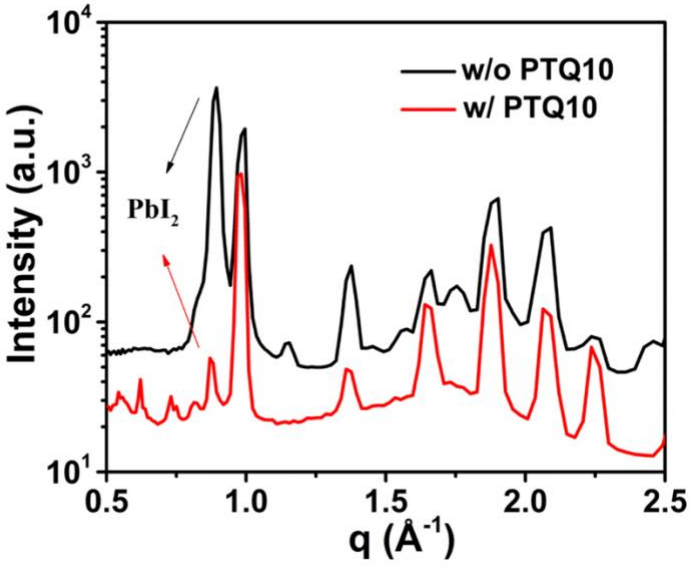

Figure S7. 1-D X-ray diffraction peaks deduced from the GIWAXS analysis.

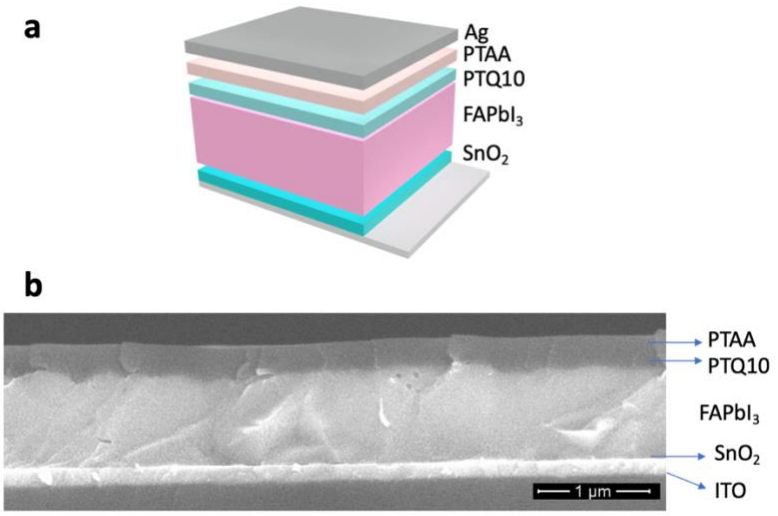

Figure S8. (a) Schematics of device structure. (b) Cross-sectional SEM images of the n-i-p structure.

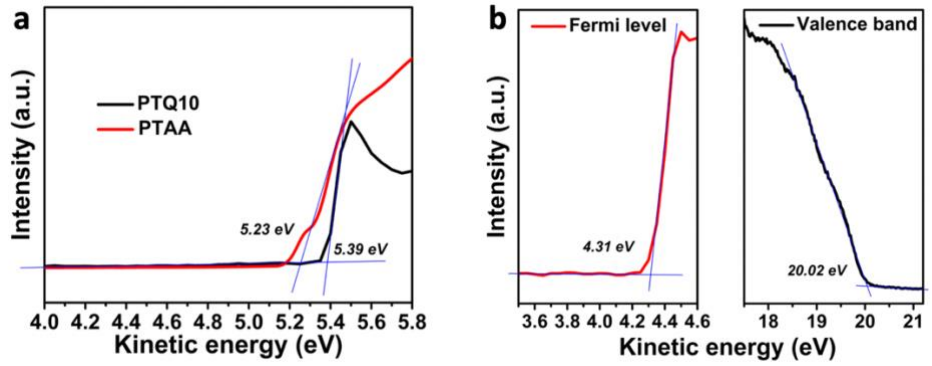

Figure S9. Ultraviolet photoelectron spectroscopy (UPS) determination of energy levels of (a) HTLs and (b) fermi level and VBM of perovskite.

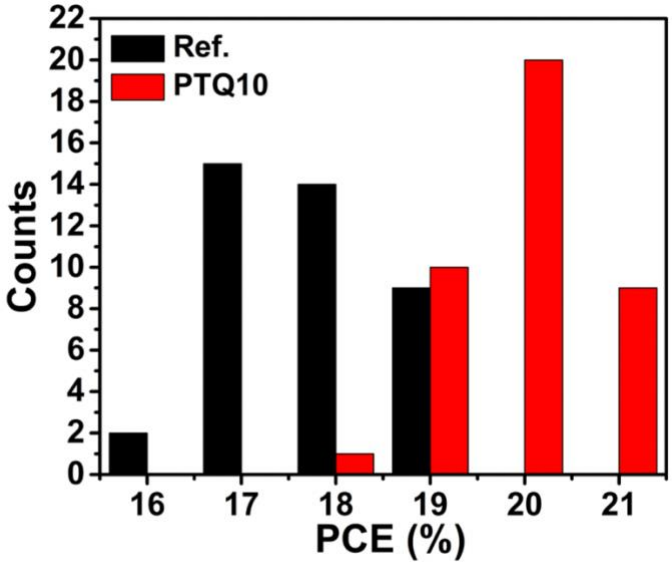

Figure S10. PCE distribution of selected 40 devices.

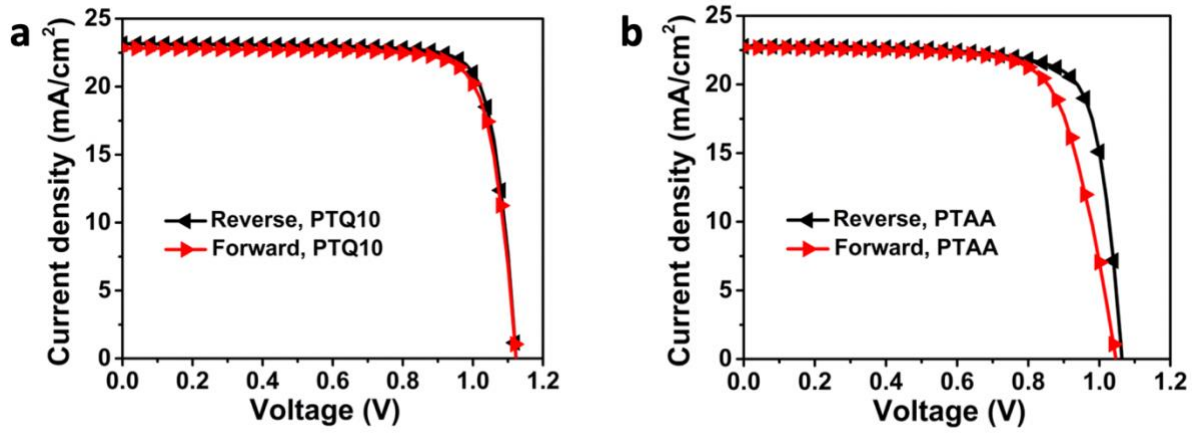

Figure S11. Hysteresis behavior of (a) target and (b) control devices. Photovoltaic performance and *J-V* measurements are based on reverse (1.2 V ⟶ 0 V, step 0.02 V) and forward scans (0 V ⟶ 1.2 V, step 0.02 V), respectively.

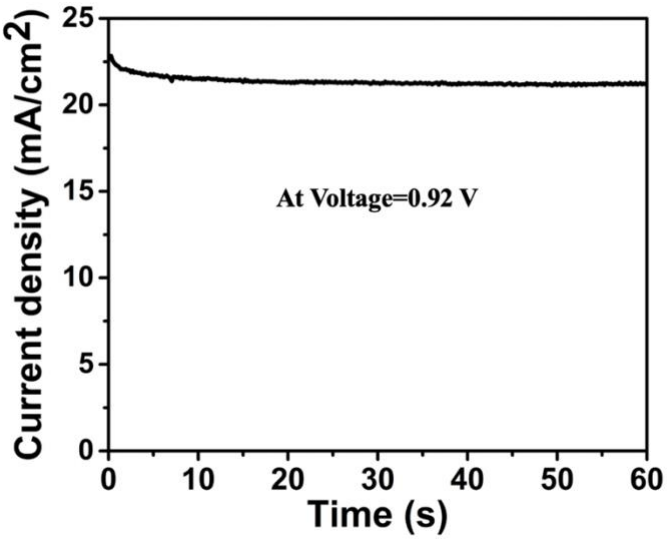

Figure S12. Steady-state PCE measurement of control device with only PTAA as HTL.

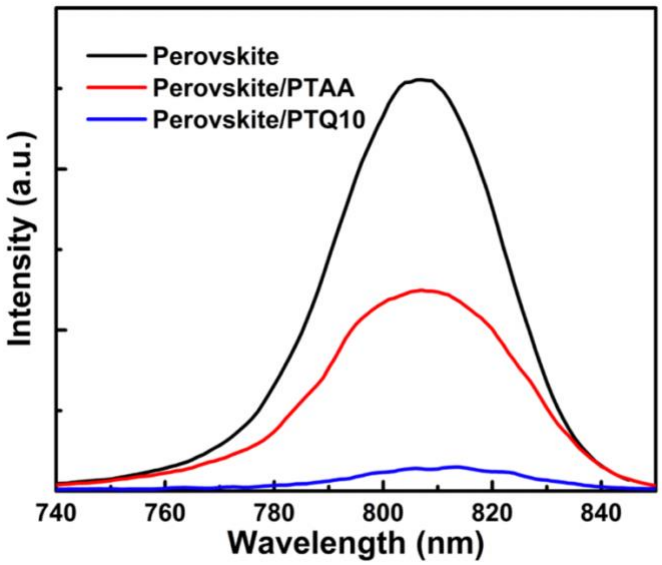

Figure S13. Steady-state PL spectra of bare perovskite film and the ones with PTAA and PTQ10 capping layer.

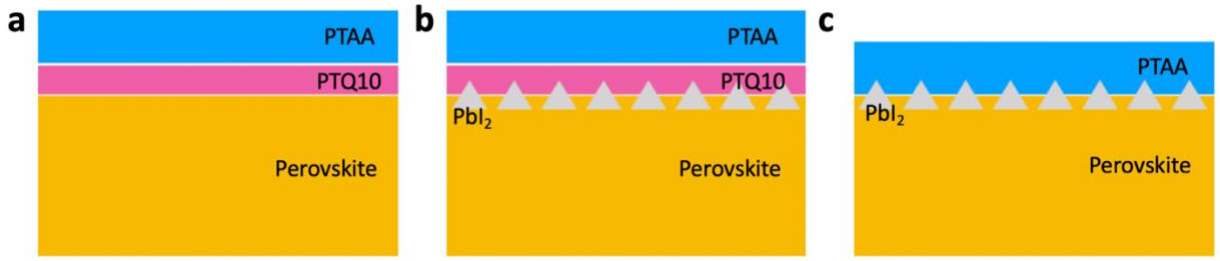

Figure S14. Schematic illustration of three different types of devices prepared. (a) ITO/SnO_2/$FAPbI_3$/PTQ10/PTAA/Ag (perovskite was treated with PTQ10 during film formation). (b) ITO/SnO_2/$FAPbI_3$/PTQ10/PTAA/Ag (perovskite with PTQ10 coated after normal film formation w/o treatment). (c) ITO/SnO_2/$FAPbI_3$/PTAA/Ag (control devices).

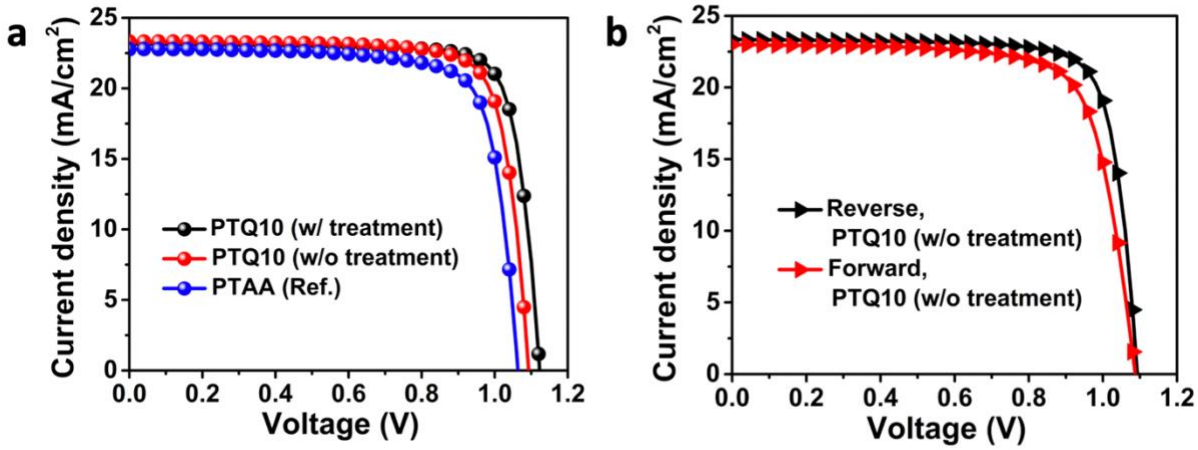

Figure S15. (a) Photovoltaic performance and *J-V* curves of three types of devices (ITO/SnO_2/$FAPbI_3$/PTQ10/PTAA/Ag (perovskite treated with PTQ10), ITO/SnO_2/$FAPbI_3$/PTQ10/PTAA/Ag (perovskite with PTQ10 but w/o treatment), ITO/SnO_2/$FAPbI_3$/PTAA/Ag (control devices)). (b) Hysteresis behavior of device with PTQ10 but no treatment.

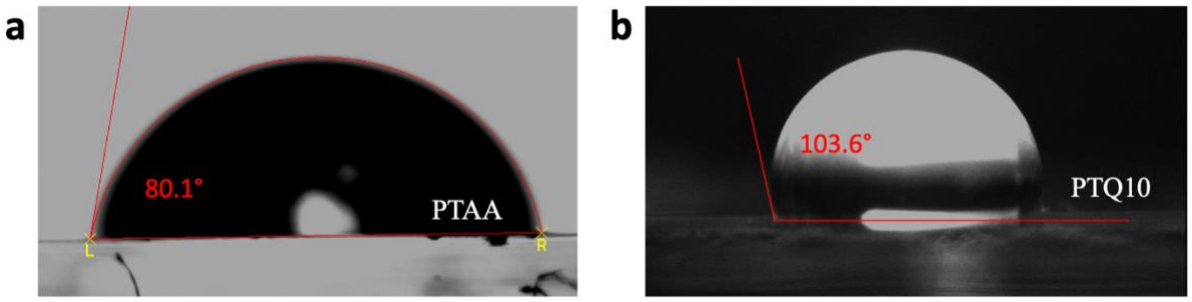

Figure S16. Wetting angles of water on the surfaces of (a) PTAA and (b) PTQ10 films.

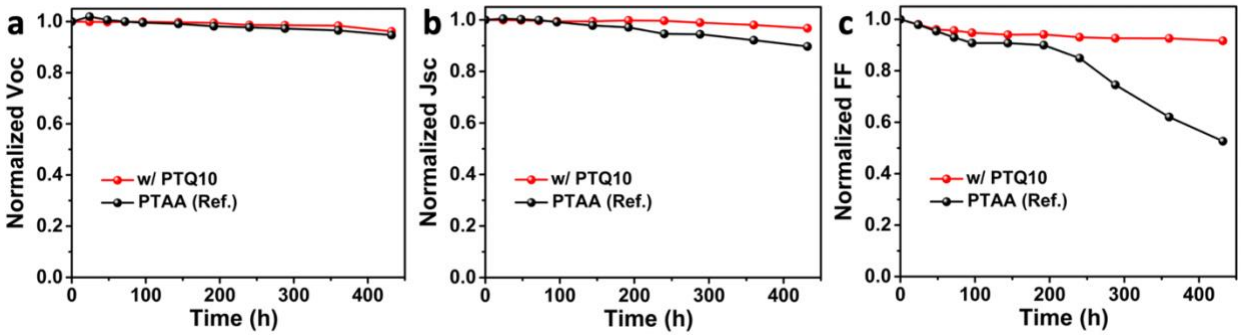

Figure S17. Devices thermal stability upon 85°C continuous annealing in nitrogen box. Detailed parameters of performance regards (a) V_{oc}, (b) J_{sc} and (c) FF.

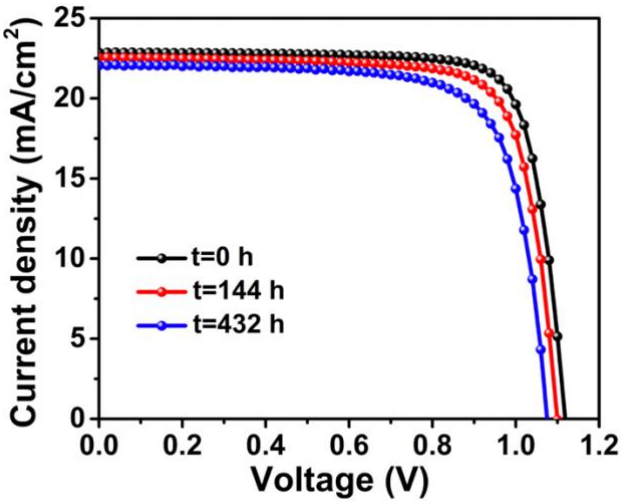

Figure S18. *J-V* curves of aged PTQ10 treated devices at 85°C after different period of time (initial, 144 h and 432 h).

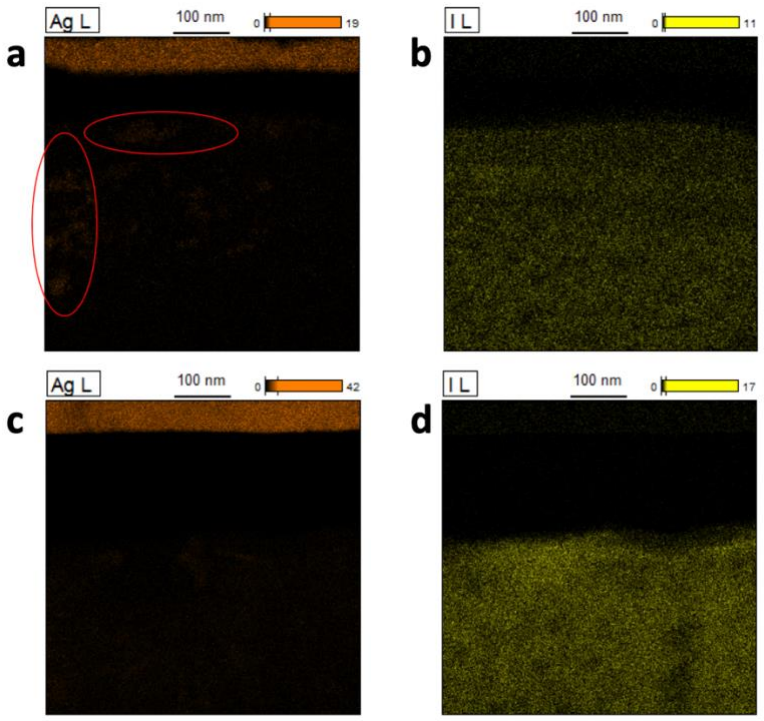

Figure S19. Energy dispersive X-ray (EDX) elemental mapping of cross-section of devices aged at 85°C. (a, b) Lead and iodine mapping of devices with only PTAA as HTL. (c, d) Lead and iodine mapping of devices adopting PTQ10 and PTAA as double HTLs.

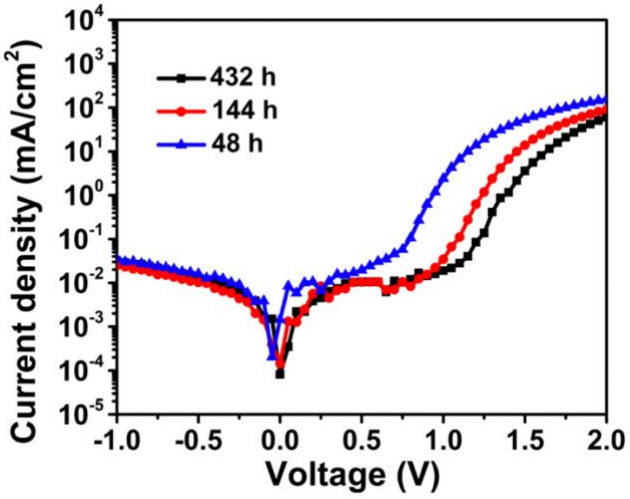

Figure S20. Dark *J-V* curves of aged devices at 85°C after different period of time.

Table S1. Photovoltaic performance of the (a) ITO/SnO_2/$FAPbI_3$/PTQ10/PTAA/Ag (perovskite was treated with PTQ10 during film formation), (b) ITO/SnO_2/$FAPbI_3$/PTQ10/PTAA/Ag (perovskite with PTQ10 coated after normal film formation w/o treatment) and (c) ITO/SnO_2/$FAPbI_3$/PTAA/Ag (control devices) from *J-V* measurements based on reverse (1.2 V ⟶ 0 V, step 0.02 V) and forward scans (0 V ⟶ 1.2 V, step 0.02 V).

	V_{oc} (V)	J_{sc} (mA/cm^2)	FF (%)	PCE (%)	Hysteresis-index (%)
PTQ10 w/CPC (Reverse)	1.12	23.15	81.57	21.21	2.97
PTQ10 w/CPC (forward)	1.12	22.84	80.24	20.58	
PTQ10 w/o CPC (Reverse)	1.09	23.33	79.70	20.32	8.21
PTQ10 w/o CPC (forward)	1.08	22.98	74.62	18.65	
PTAA (Reverse)	1.06	22.77	78.09	18.91	8.83
PTAA (Forward)	1.05	22.69	72.34	17.24	